
Are Spiking Neural Networks more expressive than Artificial Neural Networks?

Anonymous Author(s)

Affiliation

Address

email

Abstract

1 This article studies the expressive power of spiking neural networks with firing-time-
2 based information encoding, highlighting their potential for future energy-efficient
3 AI applications when deployed on neuromorphic hardware. The computational
4 power of a network of spiking neurons has already been studied via their capability
5 of approximating any continuous function. By using the Spike Response Model as
6 a mathematical model of a spiking neuron and assuming a linear response function,
7 we delve deeper into this analysis and prove that spiking neural networks generate
8 continuous piecewise linear mappings. We also show that they can emulate any
9 multi-layer (ReLU) neural network with similar complexity. Furthermore, we prove
10 that the maximum number of linear regions generated by a spiking neuron scales
11 exponentially with respect to the input dimension, a characteristic that distinguishes
12 it significantly from an artificial (ReLU) neuron. Our results further extend the
13 understanding of the approximation properties of spiking neural networks and open
14 up new avenues where spiking neural networks can be deployed instead of artificial
15 neural networks without any performance loss.

16 1 Introduction

17 Despite the remarkable success of deep neural networks (ANNs) [12], the downside of training
18 and inferring on large deep neural networks implemented on classical digital hardware lies in their
19 substantial time and energy consumption [23]. The rapid advancement in the field of neuromorphic
20 computing allows for both analog and digital computation, energy-efficient computational operations,
21 and faster inference ([21], [2]). In practice, a neuromorphic computer is typically programmed by
22 deploying a network of spiking neurons (SNNs) [21], i.e., programs are defined by the structure and
23 parameters of the neural network rather than explicit instructions.

24 SNNs are more biologically realistic as compared to ANNs, as they involve neurons transmitting
25 information asynchronously through spikes to other neurons [9]. Different encoding schemes enable
26 spiking neurons to represent analog-valued inputs, broadly categorized into rate coding (spike count)
27 and temporal coding (spike time) ([8], [17]). In this work, we assume that information is encoded in
28 the precise timing of a spike. The event-driven nature and the sparse information propagation through
29 relatively few spikes enhance system efficiency by lowering computational demands and improving
30 energy efficiency.

31 It is intuitively clear that the described differences in the processing of the information between
32 ANNs and SNNs should also lead to differences in the computations performed by these models.
33 Several groups have analyzed the expressive power of ANNs from the perspective of approximation
34 theory ([24], [4], [11], [20]) and by quantifying the number of the linear regions ([10], [18]). At
35 the same time, few attempts have been made that aim to understand the computational power of
36 SNNs. ([13], [3]) showed that continuous functions can be approximated to arbitrary precision using

37 SNNs in temporal coding. It has also been shown that spiking neurons can emulate Turing machines,
 38 arbitrary threshold circuits, and sigmoidal neurons ([15], [16]).

39 In the simplest of settings considered in [14], there remains a lack of a comprehensive theory that
 40 completely quantifies the approximation capabilities of SNNs. In an attempt to follow up along the
 41 lines of previous works ([14], [18], [22], [19]), we aim to extend the theoretical understanding that
 42 characterizes the differences and similarities in the expressive power between a network of spiking
 43 and artificial neurons employing a piecewise-linear activation function. Specifically, we aim to
 44 determine if SNNs possess the same level of expressiveness as ANNs in their ability to approximate
 45 various function spaces and in terms of the number of linear regions they can generate. The main
 46 results in Section 3 are centered around the comparison of expressive power between SNNs and
 47 ANNs.

48 2 Spiking neural networks

49 In neuroscience literature, several mathematical models exist that describe the generation and propa-
 50 gation of action-potentials. To study the expressivity of SNNs, the main principles of a spiking neuron
 51 are condensed into a (simplified) mathematical model, where certain details about the biophysics of a
 52 biological neuron are neglected. In this work, to analyze SNNs, we employ the noise-free version of
 53 the Spike Response Model (SRM) [7]. We assume a linear response function, where additionally
 54 each neuron spikes at most once to encode information through precise spike timing. This in turn
 55 simplifies the model and also makes the mathematical analysis more feasible for larger networks as
 56 compared to other models where spike dynamics are described by differential equations.

57 **Definition 1.** A spiking neural network Φ is a (simple) finite directed graph (V, E) and consists of
 58 a finite set V of spiking neurons, a subset $V_{in} \subset V$ of input neurons, a subset $V_{out} \subset V$ of output
 59 neurons, and a set $E \subset V \times V$ of synapses. Each synapse $(u, v) \in E$ is associated with a synaptic
 60 weight $w_{uv} \geq 0$, a synaptic delay $d_{uv} \geq 0$, and a response function $\varepsilon_{uv} : \mathbb{R}^+ \rightarrow \mathbb{R}$. Each neuron
 61 $v \in V \setminus V_{in}$ is associated with a firing threshold $\theta_v > 0$, and a membrane potential $P_v : \mathbb{R} \rightarrow \mathbb{R}$,

$$P_v(t) := \sum_{(u,v) \in E} \sum_{t_u^f \in F_u} w_{uv} \varepsilon_{uv}(t - t_u^f), \quad (1)$$

62 where $F_u := \{t_u^f : 1 \leq f \leq n \text{ for some } n \in \mathbb{N}\}$ denotes the set of firing times of a neuron u , i.e.,
 63 times t whenever $P_u(t)$ reaches θ_u from below.

64 In general, the membrane potential also includes the *threshold function* $\Theta_v : \mathbb{R}^+ \rightarrow \mathbb{R}^+$, that models
 65 the refractoriness effect. However, we assume that each neuron fires at most once, i.e., information
 66 is encoded in the firing time of single spikes. Thus, in Definition 1, the refractoriness effect can
 67 be ignored and the contribution of Θ_v is modelled by the constant θ_v . Moreover, the single spike
 68 condition simplifies (1) to

$$P_v(t) = \sum_{(u,v) \in E} w_{uv} \varepsilon_{uv}(t - t_u), \quad \text{where } t_u = \inf_{t \geq \min_{(z,u) \in E} \{t_z + d_{zu}\}} P_u(t) \geq \theta_u. \quad (2)$$

69 The *response function* ε_{uv} models the impact of a spike from a presynaptic neuron u on the membrane
 70 potential of a postsynaptic neuron v [7]. A biologically realistic approximation of ε_{uv} is a delayed α
 71 function [7], which is non-linear and leads to intractable problems when analyzing the propagation of
 72 spikes through an SNN. Hence, following [15], we consider a simplified response and only require
 73 ε_{uv} to satisfy the following condition:

$$\varepsilon_{uv}(t) = \begin{cases} 0, & \text{if } t \notin [d_{uv}, d_{uv} + \delta], \\ s \cdot (t - d_{uv}), & \text{if } t \in [d_{uv}, d_{uv} + \delta], \end{cases} \quad \text{where } s \in \{+1, -1\} \text{ and } \delta > 0. \quad (3)$$

74 The parameter δ is some constant assumed to be the length of a linear segment of the response
 75 function. The variable s reflects the fact that biological synapses are either *excitatory* or *inhibitory*
 76 and the *synaptic delay* d_{uv} is the time required for a spike to travel from u to v . Inserting condition
 77 (3) in (2) and setting $w_{uv} := s \cdot w_{uv}$, i.e., allowing w_{uv} to take arbitrary values in \mathbb{R} , yields

$$P_v(t) = \sum_{(u,v) \in E} \mathbf{1}_{\{0 < t - t_u - d_{uv} \leq \delta\}} w_{uv} (t - t_u - d_{uv}), \quad \text{where } t_u = \inf_{t \geq \min_{(z,u) \in E} \{t_z + d_{zu}\}} P_u(t) \geq \theta_u. \quad (4)$$

78 **2.1 Computation in terms of firing time**

79 Using (4) enables us to iteratively compute the firing time t_v of each neuron $v \in V \setminus V_{\text{in}}$ if we know
80 the firing time t_u of each neuron $u \in V$ with $(u, v) \in E$ by solving for t in

$$t \geq \inf_{(u,v) \in E} \{t_u + d_{uv}\} P_v(t) = \inf_{(u,v) \in E} \{t_u + d_{uv}\} \sum_{(u,v) \in E} \mathbf{1}_{\{0 < t - t_u - d_{uv} \leq \delta\}} w_{uv} (t - t_u - d_{uv}) = \theta_v. \quad (5)$$

81 Set $E(\mathbf{t}_U) := \{(u, v) \in E : d_{uv} + t_u < t_v \leq d_{uv} + t_u + \delta\}$, where $\mathbf{t}_U := (t_u)_{(u,v) \in E}$ is a vector
82 containing the given firing times of the presynaptic neurons. The firing time t_v satisfies

$$\theta_v = \sum_{(u,v) \in E} \mathbf{1}_{\{0 < t - t_u - d_{uv} \leq \delta\}} w_{uv} (t_v - t_u - d_{uv}) = \sum_{(u,v) \in E(\mathbf{t}_U)} w_{uv} (t_v - t_u - d_{uv}), \quad (6)$$

83

$$\text{i.e., } t_v = \frac{\theta_v}{\sum_{(u,v) \in E(\mathbf{t}_U)} w_{uv}} + \frac{\sum_{(u,v) \in E(\mathbf{t}_U)} w_{uv} (t_u + d_{uv})}{\sum_{(u,v) \in E(\mathbf{t}_U)} w_{uv}}. \quad (7)$$

84 Here, $E(\mathbf{t}_U)$ identifies the presynaptic neurons that actually have an effect on t_v based on \mathbf{t}_U . For
85 instance, if $t_w > t_v$ for some synapse $(w, v) \in E$, then w did not contribute to the firing of v since
86 the spike from w arrived after v already fired so that $(w, v) \notin E(\mathbf{t}_U)$. Equation (7) shows that t_v
87 is a weighted sum (up to a positive constant) of the firing times of neurons u with $(u, v) \in E(\mathbf{t}_U)$.
88 Flexibility, i.e., non-linearity, in this model is provided through the variation of the set $E(\mathbf{t}_U)$.
89 Depending on the firing time of the presynaptic neurons \mathbf{t}_U and the associated parameters (weights,
90 delays, threshold), $E(\mathbf{t}_U)$ contains a set of different synapses so that t_v via (7) alters accordingly.

91 We formally define SNNs and ANNs by a sequence of their parameters and their corresponding
92 realizations in Appendix A.1. To employ an SNN, the (typically analog) input information needs to
93 be encoded in the firing times of the neurons in the input layer, and similarly, the firing times of the
94 output neurons need to be translated back to an appropriate target domain. The encoding scheme
95 in Definition 3 in Appendix A.1 translates analog information into firing times and vice versa in a
96 continuous manner. Note that the following results are valid within the aforementioned setting.

97 **3 Main results**

98 A broad class of ANNs based on a wide range of activation functions such as ReLU generate
99 Continuous Piecewise Linear (CPWL) mappings ([6], [5]). In other words, these ANNs partition the
100 input domain into regions, the so-called linear regions, on which an affine function represents the
101 ANN's realization. The result in Theorem 1 shows that SNNs also express CPWL mappings under
102 very general conditions.

103 **Theorem 1.** *Any SNN Φ realizes a CPWL function provided that the sum of synaptic weights of each*
104 *neuron is positive and the encoding scheme is a CPWL function.*

105 *Proof.* We show in the Appendix (see Theorem 5) that the firing time of a spiking neuron with
106 arbitrarily many input neurons is a CPWL function with respect to the input under the assumption
107 that the sum of its weight is positive. Since Φ consists of spiking neurons arranged in layers it
108 immediately follows that each layer realizes a CPWL mapping. Thus, as a composition of CPWL
109 mappings, Φ itself realizes a CPWL function provided that the input and output encoding are also
110 CPWL functions. \square

111 Next, we show that an SNN has the capacity to effectively reproduce the output of any (ReLU) ANN.
112 In order to accurately realize the output of a ReLU network, the initial step involves realizing the
113 ReLU activation function. Despite the fact that ReLU is a very basic CPWL function, we remark that
114 it is not straightforward to realize ReLU via SNNs.

115 **Theorem 2.** *Let $a < 0 < b$. There does not exist a one-layer SNN that realizes $\sigma(x) = \max(0, x)$*
116 *on $[a, b]$. However, σ can be realized by a two-layer SNN on $[a, b]$.*

117 The proof is constructive, and we refer to Appendix A.4 for a detailed proof. Next, we extend the
118 realization of a ReLU neuron to the entire network. We only provide a short proof sketch; the details
119 are deferred to the Appendix A.5.

120 **Theorem 3.** Let $L, d \in \mathbb{N}$, $[a, b]^d \subset \mathbb{R}^d$ and let Ψ be an arbitrary ANN of depth L and fixed width d
 121 employing a ReLU non-linearity, and having a one-dimensional output. Then, there exists an SNN Φ
 122 with $N(\Phi) = N(\Psi) + L(2d + 3) - (2d + 2)$ and $L(\Phi) = 3L - 2$ that realizes \mathcal{R}_Ψ on $[a, b]^d$.

123 *Sketch of proof.* Any multi-layer ANN with ReLU activation is simply an alternating composition
 124 of affine-linear functions and a non-linear function represented by ReLU. To realize the mapping
 125 generated by some arbitrary ANN, it suffices to realize the composition of affine-linear functions and
 126 the ReLU non-linearity and then extend the construction to the whole network using concatenation
 127 and parallelization operations defined in Appendix A.2. \square

128 The aforementioned result can be generalized to ANNs with varying widths that employ any type of
 129 piecewise linear activation function. Our expressivity result in Theorem 3 implies that SNNs can
 130 essentially approximate any function with the same accuracy and (asymptotic) complexity bounds as
 131 (deep) ANNs employing a piecewise linear activation function, given the response function satisfies
 132 the introduced basic assumptions. The number of linear regions is another measure of expressivity
 133 that describes how well a neural network can fit a family of functions. The following result establishes
 134 the number of linear regions generated by a one-layer SNN.

135 **Theorem 4.** Let Φ be a one-layer SNN with a single output neuron v and d input neurons u_1, \dots, u_d
 136 such that $\sum_{i=1}^d w_{u_i v} > 0$. Then Φ partitions the input domain into at most $2^d - 1$ linear regions. In
 137 particular, for a sufficiently large input domain, the maximal number of linear regions is attained if
 138 and only if all synaptic weights are positive.

139 *Proof.* The maximum number of regions directly corresponds to $E(\mathbf{t}_U)$ defined in (7). Recall that
 140 $E(\mathbf{t}_U)$ identifies the presynaptic neurons that based on their firing times $\mathbf{t}_U = (t_{u_i})_{i=1}^d$ triggered
 141 the firing of v at time t_v . Therefore, each region in the input domain is associated to a subset of
 142 input neurons that is responsible for the firing of v on this specific domain. Hence, the number
 143 of regions is bounded by the number of non-empty subsets of $\{u_1, \dots, u_d\}$, i.e., $2^d - 1$. Now,
 144 observe that any subset of input neurons can cause a spike in v if and only if the sum of their
 145 weights is positive. Otherwise, the corresponding input region either does not exist or inputs from
 146 the corresponding region do not trigger a spike in v since they can not increase the potential $P_v(t)$
 147 as their net contribution is negative, i.e., the potential does not reach the threshold θ_v . Hence, the
 148 maximal number of regions is attained if and only if all weights are positive and thereby the sum of
 149 weights of any subset of input neurons is positive as well. \square

150 One-layer ReLU-ANNs and one-layer SNNs with one output neuron both partition the input domain
 151 into linear regions. A one-layer ReLU-ANN will partition the input domain into at most two linear
 152 regions, independent of the dimension of the input. In contrast, for a one-layer SNN, the maximum
 153 number of linear regions scales exponentially in the input dimension. This distinct behaviour stems
 154 from the intrinsic non-linearity of SNNs, originating from the subset of neurons affecting the output
 155 neuron's firing time, while in ANNs a non-linear function is applied to the output of neurons. Our
 156 result in Theorem 4 suggests that a shallow SNN can be as expressive as a deep ReLU network in
 157 terms of the number of linear regions required to express certain types of CPWL functions.

158 4 Discussion

159 The central aim of this paper is to study and compare the expressive power of SNNs and ANNs
 160 employing any piecewise linear activation function. The imperative role of time in biological neural
 161 systems accounts for differences in computation between SNNs and ANNs. The key difference in the
 162 realization of arbitrary CPWL mappings is the necessary size and complexity of the respective ANN
 163 and SNN. Recall that realizing the ReLU activation via SNNs required more computational units
 164 than the corresponding ANN (see Theorem 2). Conversely, using SNNs (see Theorem 4), one can
 165 also realize certain CPWL functions with fewer number of computational units and layers compared
 166 to ReLU-based ANNs. While neither model is clearly beneficial in terms of network complexity to
 167 express all CPWL functions, each model has distinct advantages and disadvantages. The significance
 168 of our results lies in investigating theoretically the approximation and expressivity capabilities of
 169 SNNs, highlighting their potential as an alternative computational model for complex tasks. The
 170 insights obtained from this work can further aid in designing architectures that can be implemented
 171 on neuromorphic hardware for energy-efficient applications.

References

- 172
- 173 [1] J. Berner, P. Grohs, G. Kutyniok, and P. Petersen. The modern mathematics of deep learning. In
174 *Mathematical Aspects of Deep Learning*, pages 1–111. Cambridge University Press, dec 2022.
175 doi: 10.1017/9781009025096.002.
- 176 [2] D. V. Christensen, R. Dittmann, B. Linares-Barranco, A. Sebastian, M. Le Gallo, A. Redaelli,
177 S. Slesazeck, T. Mikolajick, S. Spiga, S. Menzel, I. Valov, G. Milano, C. Ricciardi, S.-J. Liang,
178 F. Miao, M. Lanza, T. J. Quill, S. T. Keene, A. Salleo, J. Grollier, D. Markovic, A. Mizrahi,
179 P. Yao, J. J. Yang, G. Indiveri, J. P. Strachan, S. Datta, E. Vianello, A. Valentian, J. Feldmann,
180 X. Li, W. H. Pernice, H. Bhaskaran, S. Furber, E. Neftci, F. Scherr, W. Maass, S. Ramaswamy,
181 J. Tapson, P. Panda, Y. Kim, G. Tanaka, S. Thorpe, C. Bartolozzi, T. A. Cleland, C. Posch,
182 S.-C. Liu, G. Panuccio, M. Mahmud, A. N. Mazumder, M. Hosseini, T. Mohsenin, E. Donati,
183 S. Tolu, R. Galeazzi, M. E. Christensen, S. Holm, D. Ielmini, and N. Prysds. 2022 Roadmap on
184 Neuromorphic Computing and Engineering. *Neuromorph. Comput. Eng.*, 2(2), 2022.
- 185 [3] I. M. Comsa, K. Potempa, L. Versari, T. Fischbacher, A. Gesmundo, and J. Alakuijala. Temporal
186 coding in spiking neural networks with alpha synaptic function. In *ICASSP 2020 - 2020 IEEE*
187 *International Conference on Acoustics, Speech and Signal Processing (ICASSP)*, pages 8529–
188 8533, 2020. doi: 10.1109/ICASSP40776.2020.9053856.
- 189 [4] G. V. Cybenko. Approximation by superpositions of a sigmoidal function. *Mathematics of*
190 *Control, Signals and Systems*, 2:303–314, 1989.
- 191 [5] R. DeVore, B. Hanin, and G. Petrova. Neural network approximation. *Acta Numerica*, 30:
192 327–444, 2021. doi: 10.1017/S0962492921000052.
- 193 [6] N. Dym, B. Sober, and I. Daubechies. Expression of fractals through neural network functions.
194 *IEEE Journal on Selected Areas in Information Theory*, 1(1):57–66, 2020. doi: 10.1109/JSAIT.
195 2020.2991422.
- 196 [7] W. Gerstner. Time structure of the activity in neural network models. *Phys. Rev. E*, 51:738–758,
197 1995.
- 198 [8] W. Gerstner and J. van Hemmen. How to describe neuronal activity: Spikes, rates, or assemblies?
199 In *Advances in Neural Information Processing Systems*, volume 6. Morgan-Kaufmann, 1993.
- 200 [9] W. Gerstner, W. M. Kistler, R. Naud, and L. Paninski. *Neuronal Dynamics: From Single*
201 *Neurons to Networks and Models of Cognition*. Cambridge University Press, 2014.
- 202 [10] A. Goujon, A. Etemadi, and M. A. Unser. The role of depth, width, and activation complexity
203 in the number of linear regions of neural networks. *ArXiv*, abs/2206.08615, 2022.
- 204 [11] I. Gühring, M. Raslan, and G. Kutyniok. Expressivity of deep neural networks.
205 *arXiv:2007.04759*, 2020.
- 206 [12] Y. LeCun, Y. Bengio, and G. Hinton. Deep learning. *Nature*, 521(7553):436–444, 2015.
- 207 [13] W. Maass. An efficient implementation of sigmoidal neural nets in temporal coding with noisy
208 spiking neurons. Technical report, Technische Universität Graz, 1995.
- 209 [14] W. Maass. Networks of spiking neurons: The third generation of neural network models.
210 *Electron. Colloquium Comput. Complex.*, 3, 1996.
- 211 [15] W. Maass. Noisy spiking neurons with temporal coding have more computational power than
212 sigmoidal neurons. In *Advances in Neural Information Processing Systems*, volume 9. MIT
213 Press, 1996.
- 214 [16] W. Maass. Lower bounds for the computational power of networks of spiking neurons. *Neural*
215 *Computation*, 8(1):1–40, 1996. doi: 10.1162/neco.1996.8.1.1.
- 216 [17] W. Maass. On the relevance of time in neural computation and learning. *Theoretical Computer*
217 *Science*, 261(1):157–178, 2001. ISSN 0304-3975.

- 218 [18] G. Montúfar, R. Pascanu, K. Cho, and Y. Bengio. On the number of linear regions of deep
219 neural networks. In *Proceedings of the 27th International Conference on Neural Information*
220 *Processing Systems - Volume 2*, NIPS’14, page 2924–2932, Cambridge, MA, USA, 2014. MIT
221 Press.
- 222 [19] H. Mostafa, V. Ramesh, and G. Cauwenberghs. Deep supervised learning using local errors.
223 *Frontiers in Neuroscience*, 12, 2018.
- 224 [20] P. Petersen and F. Voigtlaender. Optimal approximation of piecewise smooth functions using
225 deep relu neural networks. *Neural Networks*, 108:296–330, 2018. ISSN 0893-6080.
- 226 [21] C. D. Schuman, S. R. Kulkarni, M. Parsa, J. P. Mitchell, P. Date, and B. Kay. Opportunities for
227 neuromorphic computing algorithms and applications. *Nature Computational Science*, 2(1):
228 10–19, 2022.
- 229 [22] A. Stanojevic, S. Woźniak, G. Bellec, G. Cherubini, A. Pantazi, and W. Gerstner. An exact
230 mapping from ReLU networks to spiking neural networks. *arXiv:2212.12522*, 2022.
- 231 [23] N. C. Thompson, K. Greenewald, K. Lee, and G. F. Manso. Deep learning’s diminishing returns:
232 The cost of improvement is becoming unsustainable. *IEEE Spectrum*, 58(10):50–55, 2021.
- 233 [24] D. Yarotsky. Error bounds for approximations with deep relu networks. *Neural Networks*, 94:
234 103–114, 2017. ISSN 0893-6080. doi: <https://doi.org/10.1016/j.neunet.2017.07.002>.

235 A Appendix

236 **Outline** We start by defining spiking and artificial neural networks and encoding scheme used in
237 Section A.1. Subsequently, we introduce the spiking network calculus in Section A.2 to compose
238 and parallelize different networks. In Section A.3, we provide the proof of Theorem 5. The proof of
239 Theorem 2 is given in Section A.4. Finally, in Section A.5, we prove that an SNN can realize the
240 output of any ReLU network.

241 A.1 Input and output encoding

242 By restricting our framework of SNNs to acyclic graphs, we can arrange the underlying graph in
243 layers and equivalently represent SNNs by a sequence of their parameters. This is analogous to the
244 common representation of feedforward ANNs via a sequence of matrix-vector tuples [1], [20].

245 **Definition 2.** Let $L \in \mathbb{N}$. A spiking neural network Φ associated to the acyclic graph (V, E) is a
246 sequence of matrix-matrix-vector tuples

$$\Phi = ((W^1, D^1, \Theta^1), (W^2, D^2, \Theta^2), \dots, (W^L, D^L, \Theta^L))$$

247 where $N_0, \dots, N_L \in \mathbb{N}$ and each $W^l \in \mathbb{R}^{N_{l-1} \times N_l}$, $D^l \in \mathbb{R}_+^{N_{l-1} \times N_l}$, and $\Theta^l \in \mathbb{R}_+^{N_l}$. The matrix
248 entries W_{uv}^l and D_{uv}^l represent the weight and delay value associated with the synapse $(u, v) \in E$,
249 respectively, and the entry Θ_v^l is the firing threshold associated with node $v \in V$. N_0 is the input
250 dimension and N_L is the output dimension of Φ . We call $N(\Phi) := \sum_{j=0}^L N_j$ the number of neurons
251 and $L(\Phi) := L$ denotes the number of layers of Φ .

252 **Remark 1.** In an ANN, the input signal is propagated in a synchronized manner layer-wise through
253 the network (see Definition 5). In contrast, in an SNN, information is transmitted via spikes, where
254 spikes from layer $l - 1$ affect the membrane potential of layer l neurons, resulting in asynchronous
255 propagation due to variable firing times among neurons.

256 To employ an SNN, the (typically analog) input information needs to be encoded in the firing times
257 of the neurons in the input layer, and similarly, the firing times of the output neurons need to be
258 translated back to an appropriate target domain. We will refer to this process as input encoding and
259 output decoding. The applied encoding scheme certainly depends on the specific task at hand and
260 the potential power and suitability of different encoding schemes is a topic that warrants separate
261 investigation on its own. Our focus in this work lies on exploring the intrinsic capabilities of SNNs,
262 rather than the specifics of the encoding scheme. Thus, we can formulate some guiding principles

263 for establishing a reasonable encoding scheme. First, the firing times of input and output neurons
 264 should encode analog information in a consistent way so that different networks can be concatenated
 265 in a well-defined manner. This enables us to construct suitable subnetworks and combine them
 266 appropriately to solve more complex tasks. Second, in the extreme case, the encoding scheme might
 267 directly contain the solution to a problem, underscoring the need for a sufficiently simple and broadly
 268 applicable encoding scheme to avoid this.

269 **Definition 3.** Let $[a, b]^d \subset \mathbb{R}^d$ and Φ be an SNN with input neurons u_1, \dots, u_d and output neurons
 270 v_1, \dots, v_n . Fix reference times $T_{in} \in \mathbb{R}^d$ and $T_{out} \in \mathbb{R}^n$. For any $x \in [a, b]^d$, we set the firing times
 271 of the input neurons to $(t_{u_1}, \dots, t_{u_d})^T = T_{in} + x$ and the corresponding firing times of the output
 272 neurons $(t_{v_1}, \dots, t_{v_n})^T = T_{out} + y$, determined via (7), encode the target $y \in \mathbb{R}^n$.

273 **Remark 2.** A bounded input range ensures that appropriate reference times can be fixed. Note that
 274 the introduced encoding scheme translates analog information into input firing times in a continuous
 275 manner. Occasionally, we will point out the effect of adjusting the scheme and we will sometimes
 276 with a slight abuse of notation refer to T_{in}, T_{out} as one-dimensional objects, i.e., $T_{in}, T_{out} \in \mathbb{R}$ which
 277 is justified if the corresponding vectors contain the same element in each dimension.

278 Next, we distinguish between a network and the target function it realizes. A network is a structured
 279 set of weights, delays and thresholds as defined in Definition 2, and the target function it realizes is
 280 the result of the asynchronous propagation of spikes through the network.

281 **Definition 4.** On $[a, b]^d \subset \mathbb{R}^d$, the realization of an SNN Φ with output neurons v_1, \dots, v_n and
 282 reference times $T_{in} \in \mathbb{R}^d$ and $T_{out} \in \mathbb{R}^n$, where $T_{out} > T_{in}$, is defined as the map $\mathcal{R}_\Phi : \mathbb{R}^d \rightarrow \mathbb{R}^n$,

$$\mathcal{R}_\Phi(x) = -T_{out} + (t_{v_1}, \dots, t_{v_n})^T.$$

283 Next, we give a corresponding definition of an ANN and its realization.

284 **Definition 5.** Let $L \in \mathbb{N}$. An artificial neural network Ψ is a sequence of matrix-vector tuples

$$\Psi = ((W^1, B^1), (W^2, B^2), \dots, (W^L, B^L)),$$

285 where $N_0, \dots, N_L \in \mathbb{N}$ and each $W^l \in \mathbb{R}^{N_{l-1} \times N_l}$ and $B^l \in \mathbb{R}^{N_l}$. N_0 and N_L are the input
 286 and output dimension of Ψ . We call $N(\Psi) := \sum_{j=0}^L N_j$ the number of neurons of the network
 287 Ψ , $L(\Psi) := L$ the number of layers of Ψ and N_l the width of Ψ in layer l . The realization of Ψ
 288 with component-wise activation function $\sigma : \mathbb{R} \rightarrow \mathbb{R}$ is defined as the map $\mathcal{R}_\Psi : \mathbb{R}^{N_0} \rightarrow \mathbb{R}^{N_L}$,
 289 $\mathcal{R}_\Psi(x) = y_L$, where y_L results from

$$y_0 = x, \quad y_l = \sigma(W^l y_{l-1} + B^l), \text{ for } l = 1, \dots, L-1, \quad \text{and } y_L = W^L y_{L-1} + B^L. \quad (8)$$

290 In the remainder, we always employ the ReLU activation function $\sigma(x) = \max(0, x)$. One can
 291 perform basic actions on neural networks such as concatenation and parallelization to construct larger
 292 networks from existing ones. Adapting a general approach for ANNs as defined in [1], [20], we
 293 formally introduce the concatenation and parallelization of networks of spiking neurons in the next
 294 Section A.2.

295 A.2 Spiking neural network calculus

296 It can be observed from Definition 3 that both inputs and outputs of SNNs are encoded in a unified
 297 format. This characteristic is crucial for concatenating/parallelizing two spiking network architectures
 298 that further enable us to attain compositions/parallelizations of network realizations.

299 We operate in the following setting: Let $L_1, L_2, d_1, d_2, d'_1, d'_2 \in \mathbb{N}$. Consider two SNNs Φ_1, Φ_2
 300 given by

$$\Phi_i = ((W_1^i, D_1^i, \Theta_1^i), \dots, (W_{L_i}^i, D_{L_i}^i, \Theta_{L_i}^i)), \quad i = 1, 2,$$

301 with input domains $[a_1, b_1]^{d_1} \subset \mathbb{R}^{d_1}$, $[a_2, b_2]^{d_2} \subset \mathbb{R}^{d_2}$ and output dimension d'_1, d'_2 , respectively.
 302 Denote the input neurons by u_1, \dots, u_{d_i} with respective firing times $t_{u_j}^i$ and the output neurons by
 303 $v_1, \dots, v_{d'_i}$ with respective firing times $t_{v_j}^i$ for $i = 1, 2$. By Definition 3, we can express the firing
 304 times of the input neurons as

$$\begin{aligned} t_u^1(x) &:= (t_{u_1}^1, \dots, t_{u_{d_1}}^1)^T = T_{in}^1 + x \quad \text{for } x \in [a_1, b_1]^{d_1}, \\ t_u^2(x) &:= (t_{u_1}^2, \dots, t_{u_{d_2}}^2)^T = T_{in}^2 + x \quad \text{for } x \in [a_2, b_2]^{d_2} \end{aligned} \quad (9)$$

305 and, by Definition 4, the realization of the networks as

$$\begin{aligned}\mathcal{R}_{\Phi_1}(x) &= -T_{\text{out}}^1 + t_v^1(t_u^1(x)) := -T_{\text{out}}^1 + (t_{v_1}^1, \dots, t_{v_{d_1}'}^1)^T \quad \text{for } x \in [a_1, b_1]^{d_1}, \\ \mathcal{R}_{\Phi_2}(x) &= -T_{\text{out}}^2 + t_v^2(t_u^2(x)) := -T_{\text{out}}^2 + (t_{v_1}^2, \dots, t_{v_{d_2}'}^2)^T \quad \text{for } x \in [a_2, b_2]^{d_2}\end{aligned}\quad (10)$$

306 for some constants $T_{\text{in}}^1 \in \mathbb{R}^{d_1}$, $T_{\text{in}}^2 \in \mathbb{R}^{d_2}$, $T_{\text{out}}^1 \in \mathbb{R}^{d_1'}$, $T_{\text{out}}^2 \in \mathbb{R}^{d_2'}$.

307 We define the concatenation of the two networks in the following way.

308 **Definition 6.** (Concatenation) Let Φ_1 and Φ_2 be such that the input layer of Φ_1 has the same
309 dimension as the output layer of Φ_2 , i.e., $d_2' = d_1$. Then, the concatenation of Φ_1 and Φ_2 , denoted as
310 $\Phi_1 \bullet \Phi_2$, represents the $(L_1 + L_2)$ -layer network

$$\Phi_1 \bullet \Phi_2 := ((W_1^2, D_1^2, \Theta_1^2), \dots, (W_{L_2}^2, D_{L_2}^2, \Theta_{L_2}^2), (W_1^1, D_1^1, \Theta_1^1), \dots, (W_{L_1}^1, D_{L_1}^1, \Theta_{L_1}^1)).$$

311 **Lemma 1.** Let $d_2' = d_1$ and fix $T_{\text{in}} = T_{\text{in}}^2$ and $T_{\text{out}} = T_{\text{out}}^1$. If $T_{\text{out}}^2 = T_{\text{in}}^1$ and $\mathcal{R}_{\Phi_2}([a_2, b_2]^{d_2}) \subset$
312 $[a_1, b_1]^{d_1}$, then

$$\mathcal{R}_{\Phi_1 \bullet \Phi_2}(x) = \mathcal{R}_{\Phi_1}(\mathcal{R}_{\Phi_2}(x)) \quad \text{for all } x \in [a, b]^{d_2}$$

313 with respect to the reference times $T_{\text{in}}, T_{\text{out}}$. Moreover, $\Phi_1 \bullet \Phi_2$ is composed of $N(\Phi_1) + N(\Phi_2) - d_1$
314 computational units.

315 *Proof.* It is straightforward to verify via the construction that the network $\Phi_1 \bullet \Phi_2$ is composed of
316 $N(\Phi_1) + N(\Phi_2) - d_1$ computational units. Moreover, under the given assumptions $\mathcal{R}_{\Phi_1} \circ \mathcal{R}_{\Phi_2}$ is
317 well-defined so that (9) and (10) imply

$$\begin{aligned}\mathcal{R}_{\Phi_1 \bullet \Phi_2}(x) &= -T_{\text{out}}^1 + t_v^1(t_v^2(T_{\text{in}} + x)) = -T_{\text{out}}^1 + t_v^1(t_v^2(T_{\text{in}}^2 + x)) = -T_{\text{out}}^1 + t_v^1(t_v^2(t_u^2(x))) \\ &= -T_{\text{out}}^1 + t_v^1(T_{\text{out}}^2 + \mathcal{R}_{\Phi_2}(x)) = -T_{\text{out}}^1 + t_v^1(T_{\text{in}}^1 + \mathcal{R}_{\Phi_2}(x)) \\ &= -T_{\text{out}}^1 + t_v^1(t_u^1(\mathcal{R}_{\Phi_2}(x))) = \mathcal{R}_{\Phi_1}(\mathcal{R}_{\Phi_2}(x)) \quad \text{for } x \in [a_2, b_2]^{d_2}.\end{aligned}$$

318 □

319 In addition to concatenating networks, we also perform parallelization operation on SNNs.

320 **Definition 7.** (Parallelization) Let Φ_1 and Φ_2 be such that they have the same depth and input
321 dimension, i.e., $L_1 = L_2 =: L$ and $d_1 = d_2 =: d$. Then, the parallelization of Φ_1 and Φ_2 , denoted
322 as $P(\Phi_1, \Phi_2)$, represents the L -layer network with d -dimensional input

$$P(\Phi_1, \Phi_2) := ((\tilde{W}_1, \tilde{D}_1, \tilde{\Theta}_1), \dots, (\tilde{W}_L, \tilde{D}_L, \tilde{\Theta}_L)),$$

323 where

$$\tilde{W}_1 = \begin{pmatrix} W_1^1 & W_1^2 \end{pmatrix}, \quad \tilde{D}_1 = \begin{pmatrix} D_1^1 & D_1^2 \end{pmatrix}, \quad \tilde{\Theta}_1 = \begin{pmatrix} \Theta_1^1 \\ \Theta_1^2 \end{pmatrix}$$

324 and

$$\tilde{W}_l = \begin{pmatrix} W_l^1 & 0 \\ 0 & W_l^2 \end{pmatrix}, \quad \tilde{D}_l = \begin{pmatrix} D_l^1 & 0 \\ 0 & D_l^2 \end{pmatrix}, \quad \tilde{\Theta}_l = \begin{pmatrix} \Theta_l^1 \\ \Theta_l^2 \end{pmatrix}, \quad \text{for } 1 < l \leq L.$$

325 **Lemma 2.** Let $d := d_2 = d_1$ and fix $T_{\text{in}} := T_{\text{in}}^1$, $T_{\text{out}} := (T_{\text{out}}^1, T_{\text{out}}^2)$, $a := a_1$ and $b := b_1$. If
326 $T_{\text{in}}^2 = T_{\text{in}}^1$, $T_{\text{out}}^2 = T_{\text{out}}^1$ and $a_1 = a_2$, $b_1 = b_2$, then

$$\mathcal{R}_{P(\Phi_1, \Phi_2)}(x) = (\mathcal{R}_{\Phi_1}(x), \mathcal{R}_{\Phi_2}(x)) \quad \text{for } x \in [a, b]^d$$

327 with respect to the reference times $T_{\text{in}}, T_{\text{out}}$. Moreover, $P(\Phi_1, \Phi_2)$ is composed of $N(\Phi_1) + N(\Phi_2) - d$
328 computational units.

329 *Proof.* The number of computational units is an immediate consequence of the construction. Since
330 the input domains of Φ_1 and Φ_2 agree, (9) and (10) show that

$$\begin{aligned}\mathcal{R}_{P(\Phi_1, \Phi_2)}(x) &= -T_{\text{out}} + (t_v^1(T_{\text{in}} + x), t_v^2(T_{\text{in}} + x)) = (-T_{\text{out}}^1 + t_v^1(T_{\text{in}}^1 + x), -T_{\text{out}}^2 + t_v^2(T_{\text{in}}^2 + x)) \\ &= (-T_{\text{out}}^1 + t_v^1(t_u^1(x)), -T_{\text{out}}^2 + t_v^2(t_u^2(x))) = (\mathcal{R}_{\Phi_1}(x), \mathcal{R}_{\Phi_2}(x)) \quad \text{for } x \in [a, b]^d.\end{aligned}$$

331 □

332 **Remark 3.** Note that parallelization and concatenation can be straightforwardly extended (re-
333 cursively) to a finite number of networks. Additionally, more general forms of parallelization and
334 concatenations of networks, e.g., parallelization of networks with different depths, can be established.
335 However, for the constructions presented in this work, the introduced notions suffice.

336 A.3 Realizations of spiking neural networks

337 In this section, we show that a spiking neuron generates a CPWL mapping.

338 **Theorem 5.** *Let v be a spiking neuron with d input neurons u_1, \dots, u_d . The firing time*
 339 *$t_v(t_{u_1}, \dots, t_{u_d})$ as a function of the firing times t_{u_1}, \dots, t_{u_d} is a CPWL mapping provided that*
 340 *$\sum_{i=1}^d w_{u_i v} > 0$, where $w_{u_i v} \in \mathbb{R}$ is the synaptic weight between u_i and v .*

341 *Proof.* The condition $\sum_{i=1}^d w_{u_i v} > 0$ simply ensures that the input domain is decomposed into
 342 regions associated with subsets of input neurons with positive net weight. If $\sum_{i=1}^d w_{u_i v} < 0$, then
 343 the corresponding input region either does not exist or inputs from the corresponding region do
 344 not trigger a spike in v since they can not increase the potential $P_v(t)$ as their net contribution is
 345 negative, i.e., the potential does not reach the threshold θ_v . Hence, with $\sum_{i=1}^d w_{u_i v} > 0$, the situation
 346 described above can not arise and the notion of a CPWL mapping on \mathbb{R}^d is well-defined. Denote the
 347 associated delays by $d_{u_i v} \geq 0$ and the threshold of v by $\theta_v > 0$. We distinguish between the $2^d - 1$
 348 variants of input combinations that can cause a firing of v . Let $I \subset \{1, \dots, d\}$ be a non-empty subset
 349 and I^c the complement of I in $\{1, \dots, d\}$, i.e., $I^c = \{1, \dots, d\} \setminus I$. Assume that all u_i with $i \in I$
 350 contribute to the firing of v whereas spikes from u_i with $i \in I^c$ do not influence the firing of v . Then
 351 $\sum_{i \in I} w_{u_i v}$ is required to be positive, and by (6) and (7) the following holds:

$$t_{u_k} + d_{u_k v} \geq t_v = \frac{\theta_v}{\sum_{i \in I} w_{u_i v}} + \sum_{i \in I} \frac{w_{u_i v}}{\sum_{j \in I} w_{u_j v}} (t_{u_i} + d_{u_i v}) \quad \text{for all } k \in I^c \quad (11)$$

352 and

$$t_{u_k} + d_{u_k v} < t_v = \frac{\theta_v}{\sum_{i \in I} w_{u_i v}} + \sum_{i \in I} \frac{w_{u_i v}}{\sum_{j \in I} w_{u_j v}} (t_{u_i} + d_{u_i v}) \quad \text{for all } k \in I. \quad (12)$$

353 Rewriting yields

$$t_{u_k} \geq \frac{\theta_v}{\sum_{i \in I} w_{u_i v}} + \sum_{i \in I} \frac{w_{u_i v}}{\sum_{j \in I} w_{u_j v}} (t_{u_i} + d_{u_i v}) - d_{u_k v} \quad \text{for all } k \in I^c \quad (13)$$

354 and

$$t_{u_k} \begin{cases} < \frac{\theta_v}{\sum_{j \in I \setminus k} w_{u_j v}} + \sum_{i \in I \setminus k} \frac{w_{u_i v}}{\sum_{j \in I \setminus k} w_{u_j v}} (t_{u_i} + d_{u_i v}) - d_{u_k v}, & \text{if } \frac{\sum_{i \in I \setminus k} w_{u_i v}}{\sum_{i \in I} w_{u_i v}} > 0 \\ > \frac{\theta_v}{\sum_{j \in I \setminus k} w_{u_j v}} + \sum_{i \in I \setminus k} \frac{w_{u_i v}}{\sum_{j \in I \setminus k} w_{u_j v}} (t_{u_i} + d_{u_i v}) - d_{u_k v}, & \text{if } \frac{\sum_{i \in I \setminus k} w_{u_i v}}{\sum_{i \in I} w_{u_i v}} < 0 \end{cases} \quad \forall k \in I.$$

355 It is now clear that the firing time $t_v(t_{u_1}, \dots, t_{u_d})$ as a function of the input t_{u_1}, \dots, t_{u_d} is a
 356 piecewise linear mapping on polytopes decomposing \mathbb{R}^d . To show that the mapping is additionally
 357 continuous, we need to assess $t_v(t_{u_1}, \dots, t_{u_d})$ on the breakpoints. Let $I, J \subset \{1, \dots, d\}$ be index
 358 sets corresponding to input neurons $\{u_i : i \in I\}, \{u_j : j \in J\}$ that cause v to fire on the input region
 359 $R^I \subset \mathbb{R}^d, R^J \subset \mathbb{R}^d$ respectively. Assume that it is possible to transition from R^I to R^J through
 360 a breakpoint $t^{I,J} = (t_{u_1}^{I,J}, \dots, t_{u_d}^{I,J}) \in \mathbb{R}^d$ without leaving $R^I \cup R^J$. Crossing the breakpoint is
 361 equivalent to the fact that the input neurons $\{u_i : i \in I \setminus J\}$ do not contribute to the firing of v
 362 anymore and the input neurons $\{u_i : i \in J \setminus I\}$ begin to contribute to the firing of v .

363 Assume first that $J \subset I$. Then, we observe that the breakpoint $t^{I,J}$ is necessarily an element of
 364 the linear region corresponding to the index set with smaller cardinality, i.e., $t^{I,J} \in R^J$. This is an
 365 immediate consequence of (12) and the fact that $t^{I,J}$ is characterized by

$$t_{u_k}^{I,J} + d_{u_k v} = t_v(t^{I,J}) \quad \text{for all } k \in I \setminus J. \quad (14)$$

366 Indeed, if $t_{u_k}^{I,J} + d_{u_k v} > t_v(t^{I,J})$, then there exists $\varepsilon_k > 0$ such that (13) also holds for $t_{u_k}^{I,J} \pm \varepsilon$,
 367 where $0 \leq \varepsilon < \varepsilon_k$, i.e., a small change in $t_{u_k}^{I,J}$ is not sufficient to change the corresponding linear
 368 region, contradicting our assumption that $t^{I,J}$ is a breakpoint.

369 The firing time $t_v(t^{I,J})$ is explicitly given by

$$t_v(t^{I,J}) = \frac{\theta_v}{\sum_{i \in J} w_{u_i v}} + \sum_{i \in J} \frac{w_{u_i v}}{\sum_{j \in J} w_{u_j v}} (t_{u_i}^{I,J} + d_{u_i v})$$

370 Using (14), we obtain

$$0 = -\frac{w_{u_k v}}{\sum_{j \in J} w_{u_j v}} (t_v(t^{I,J}) - (t_{u_k}^{I,J} + d_{u_k v})) \quad \text{for all } k \in I \setminus J$$

371 so that

$$t_v(t^{I,J}) = \frac{\theta_v}{\sum_{i \in J} w_{u_i v}} + \sum_{i \in J} \frac{w_{u_i v}}{\sum_{j \in J} w_{u_j v}} (t_{u_i}^{I,J} + d_{u_i v}) - \sum_{i \in I \setminus J} \frac{w_{u_i v}}{\sum_{j \in J} w_{u_j v}} (t_v(t^{I,J}) - (t_{u_i}^{I,J} + d_{u_i v})).$$

372 Solving for $t_v(t^{I,J})$ yields

$$\begin{aligned} t_v(t^{I,J}) &= \left(1 + \sum_{i \in I \setminus J} \frac{w_{u_i v}}{\sum_{j \in J} w_{u_j v}}\right)^{-1} \cdot \left(\frac{\theta_v}{\sum_{i \in J} w_{u_i v}} + \sum_{i \in I} \frac{w_{u_i v}}{\sum_{j \in J} w_{u_j v}} (t_{u_i}^{I,J} + d_{u_i v})\right) \\ &= \sum_{i \in J} \frac{w_{u_i v}}{\sum_{j \in I} w_{u_j v}} \cdot \left(\frac{\theta_v}{\sum_{i \in J} w_{u_i v}} + \sum_{i \in I} \frac{w_{u_i v}}{\sum_{j \in J} w_{u_j v}} (t_{u_i}^{I,J} + d_{u_i v})\right) \\ &= \frac{\theta_v}{\sum_{i \in I} w_{u_i v}} + \sum_{i \in I} \frac{w_{u_i v}}{\sum_{j \in I} w_{u_j v}} (t_{u_i}^{I,J} + d_{u_i v}), \end{aligned}$$

373 which is exactly the expression for the firing time on R^I . This shows that $t_v(t_{u_1}, \dots, t_{u_d})$ is
 374 continuous in $t^{I,J}$. Since the breakpoint $t^{I,J}$ was chosen arbitrarily, $t_v(t_{u_1}, \dots, t_{u_d})$ is continuous at
 375 any breakpoint.

376 The case $I \subset J$ follows analogously. It remains to check the case when neither $I \subset J$ nor $J \subset I$. To
 377 that end, let $i^* \in I \setminus J$ and $j^* \in J \setminus I$. Assume without loss of generality that $t^{I,J} \in R^I$ so that (11)
 378 and (12) imply

$$t_{u_{i^*}}^{I,J} + d_{u_{i^*} v} < t_v(t^{I,J}) \leq t_{u_{j^*}}^{I,J} + d_{u_{j^*} v}.$$

379 Hence, there exists $\varepsilon > 0$ such that

$$t_{u_{i^*}}^{I,J} + d_{u_{i^*} v} < t_{u_{j^*}}^{I,J} + d_{u_{j^*} v} - \varepsilon. \quad (15)$$

380 Moreover, due to the fact that $t^{I,J}$ is a breakpoint we can find $t^J \in R^J \cap \mathcal{B}(t^{I,J}; \frac{\varepsilon}{3})$, where $\mathcal{B}(t^{I,J}; \frac{\varepsilon}{3})$
 381 denotes the open ball with radius $\frac{\varepsilon}{3}$ centered at $t^{I,J}$. In particular, this entails that

$$-\frac{\varepsilon}{3} < (t_{u_{i^*}}^J - t_{u_{i^*}}^{I,J}), (t_{u_{j^*}}^{I,J} - t_{u_{j^*}}^J) < \frac{\varepsilon}{3},$$

382 and therefore together with (15)

$$\begin{aligned} t_{u_{i^*}}^J + d_{u_{i^*} v} - (t_{u_{j^*}}^J + d_{u_{j^*} v}) &= (t_{u_{i^*}}^J - t_{u_{i^*}}^{I,J}) + (t_{u_{i^*}}^{I,J} + d_{u_{i^*} v} - (t_{u_{j^*}}^{I,J} + d_{u_{j^*} v})) + (t_{u_{j^*}}^{I,J} - t_{u_{j^*}}^J) \\ &< 0, \quad \text{i.e., } t_{u_{i^*}}^J + d_{u_{i^*} v} < t_{u_{j^*}}^J + d_{u_{j^*} v}. \end{aligned}$$

383 However, (11) and (12) require that

$$t_{u_{j^*}}^J + d_{u_{j^*} v} < t_v(t^J) \leq t_{u_{i^*}}^J + d_{u_{i^*} v}$$

384 since $t^J \in R^J$. Thus, $t^{I,J}$ can not exist and the case when neither $I \subset J$ nor $J \subset I$ can not arise. \square

385 A.4 Realizing ReLU with spiking neural networks

386 **Proposition 1.** Let $c_1 \in \mathbb{R}$, $c_2 \in (a, b) \subset \mathbb{R}$ and consider $f_1, f_2 : [a, b] \rightarrow \mathbb{R}$ defined as

$$f_1(x) = \begin{cases} x + c_1 & , \text{ if } x > c_2 \\ c_1 & , \text{ if } x \leq c_2 \end{cases} \quad \text{or} \quad f_2(x) = \begin{cases} x + c_1 & , \text{ if } x < c_2 \\ c_1 & , \text{ if } x \geq c_2 \end{cases}.$$

387 There does not exist a one-layer SNN with output neuron v and input neuron u_1 such that $t_v(x) =$
 388 $f_i(x)$, $i = 1, 2$, on $[a, b]$, where $t_v(x)$ denotes the firing time of v on input $t_{u_1} = x$.

389 *Proof.* First, note that a one-layer SNN realizes a CPWL function. For $c_2 \neq 0$, f_i is not continuous
 390 and therefore can not be emulated by the firing time of any one-layer SNN. Hence, it is left to consider
 391 the case $c_2 = 0$. If u_1 is the only input neuron, then v fires if and only if $w_{u_1v} > 0$ and by (7) the
 392 firing time is given by

$$t_v(x) = \frac{\theta}{w_{u_1v}} + x + d_{u_1v} \quad \text{for all } x \in [a, b],$$

393 i.e., $t_v \neq f_i$. Therefore, we introduce auxiliary input neurons u_2, \dots, u_n and assume without loss
 394 of generality that $t_{u_i} + d_{u_iv} < t_{u_j} + d_{u_jv}$ for $j > i$. Here, the firing times t_{u_i} , $i = 2, \dots, n$, are
 395 suitable constants. We will show that even in this extended setting $t_v \neq f_i$ still holds and thereby
 396 also the claim.

397 For the sake of contradiction, assume that $t_v(x) = f_1(x)$ for all $x \in [a, b]$. This implies that there
 398 exists an index set $J \subset \{1, \dots, n\}$ with $\sum_{j \in J} w_{u_jv} > 0$ and a corresponding interval $(a_1, 0] \subset [a, b]$
 399 such that

$$c_1 = t_v(x) = \frac{1}{\sum_{i \in J} w_{u_iv}} \left(\theta_v + \sum_{i \in J} w_{u_iv} (t_{u_i} + d_{u_iv}) \right) \quad \text{for all } x \in (a_1, 0],$$

400 where we have applied (7). Moreover, J is of the form $J = \{2, \dots, \ell\}$ for some $\ell \in \{1, \dots, n\}$
 401 because $(t_{u_i} + d_{u_iv})_{i=2}^n$ is in ascending order, i.e., if the spike from u_ℓ has reached v before v fired,
 402 then so did the spikes from u_i , $2 \leq i < \ell$. Additionally, we know that $1 \notin J$ since otherwise t_v is
 403 non-constant on $(a_1, 0]$ (due to the contribution from u_1), i.e., $t_v \neq c_1$ on $(a_1, 0]$. In particular, the
 404 spike from u_1 reaches v after the neurons u_2, \dots, u_ℓ already caused v to fire, i.e., we have

$$x + d_{u_1v} \geq t_v(x) = c_1 \quad \text{for all } x \in (a_1, 0].$$

405 However, it immediately follows that

$$x + d_{u_1v} > d_{u_1v} \geq c_1 \quad \text{for all } x > 0.$$

406 Thus, we obtain $t_v(x) = c_1$ for $x > 0$ (since the spike from u_1 still reaches v only after v emitted a
 407 spike), which contradicts $t_v(x) = f_1(x)$ for all $x \in [a, b]$.

408 We perform a similar analysis to show that f_2 can not be emulated. For the sake of contradiction,
 409 assume that $t_v(x) = f_2(x)$ for all $x \in [a, b]$. This implies that there exists an index set $I \subset \{1, \dots, n\}$
 410 with $\sum_{i \in I} w_{u_iv} > 0$ and a corresponding interval $(a_2, 0) \subset [a, b]$ such that

$$x + c_1 = t_v(x) = \frac{1}{\sum_{i \in I} w_{u_iv}} \left(\theta_v + w_{u_1v} (x + d_{u_1v}) + \sum_{i \in I \setminus \{1\}} w_{u_iv} (t_{u_i} + d_{u_iv}) \right) \quad \text{for } x \in (a_2, 0), \quad (16)$$

411 where we have applied (7). We immediately observe that $1 \in I$, since otherwise t_v is constant
 412 on $(a_2, 0)$. Moreover, by the same reasoning as before we can write $I = \{1, \dots, \ell\}$ for some
 413 $\ell \in \{1, \dots, n\}$. In order for $t_v(x) = f_2(x)$ for all $x \in [a, b]$ to hold, there needs to exist an index
 414 set $J \subset \{1, \dots, n\}$ with $\sum_{j \in J} w_{u_jv} > 0$ and a corresponding interval $[0, b_2) \subset [a, b]$ such that
 415 $t_v = c_1$ on $[0, b_2)$. We conclude that $J = \{1, \dots, m\}$ or $J = \{2, \dots, m\}$ for some $m \in \{1, \dots, n\}$.
 416 In the former case, t_v is non-constant on $[0, b_2)$ (due to the contribution from u_1), i.e., $t_v \neq c_1$
 417 on $[0, b_2)$. Hence, it remains to consider the latter case. Note that $m < \ell$ implies that $b_2 \leq a_2$
 418 (as u_2, \dots, u_m already triggered a firing of v before the spike from u_ℓ arrived) contradicting the
 419 construction $a_2 < 0 < b_2$. Similarly, $m = \ell$, i.e., $J = I \setminus \{1\}$ is not valid because (16) requires that

$$\frac{w_{u_1v}}{\sum_{i \in I} w_{u_iv}} = 1 \Leftrightarrow \sum_{i \in I \setminus \{1\}} w_{u_iv} = 0 \Leftrightarrow \sum_{j \in J} w_{u_jv} = 0.$$

420 Finally, $m > \ell$ also results in a contradiction since

$$0 < \sum_{j \in J} w_{u_jv} = \sum_{i \in I \setminus \{1\}} w_{u_iv} + \sum_{j \in J \setminus I} w_{u_jv} = \sum_{j \in J \setminus I} w_{u_jv}$$

421 together with

$$0 < \sum_{i \in I} w_{u_iv} = \sum_{i \in I \setminus \{1\}} w_{u_iv} + w_{u_1v} = w_{u_1v}$$

422 imply that the neurons $\{u_j : j \in \{1\} \cup J\}$ also trigger a spike in v . However, the corresponding
 423 interval where the firing of v is caused by $\{u_j : j \in \{1\} \cup J\}$ is necessarily located between $(a_2, 0)$
 424 and $[0, b_2)$, which is not possible. \square

425 **Remark 4.** The proof shows that $-f_1$ also can not be emulated by a one-layer SNN. Moreover, by
 426 adjusting (16) we observe that a necessary condition for $-f_2$ to be realized is that

$$\sum_{i \in I} \frac{w_{u_1 v}}{w_{u_i v}} = -1 \Leftrightarrow - \sum_{i \in I \setminus \{1\}} w_{u_i v} = 2w_{u_1 v} \Leftrightarrow -\frac{1}{2} \sum_{i \in I \setminus \{1\}} w_{u_i v} = w_{u_1 v}.$$

427 Under this condition $-f_2$ can indeed be realized by a one-layer SNN as the following statement
 428 confirms.

429 **Proposition 2.** Let $a < 0 < b, c$ and consider $f : [a, b] \rightarrow \mathbb{R}$ defined as

$$f(x) = \begin{cases} -x + c & , \text{ if } x < 0 \\ c & , \text{ if } x \geq 0 \end{cases}.$$

430 There exists a one-layer SNN Φ with output neuron v and input neuron u_1 such that $t_v(x) = f(x)$ on
 431 $[a, b]$, where $t_v(x)$ denotes the firing time of v on input $t_{u_1} = x$.

432 *Proof.* We introduce an auxiliary input neuron with constant firing time $t_{u_2} \in \mathbb{R}$ and specify the
 433 parameter of $\Phi = ((W, D, \Theta))$ in the following manner (see Figure 1a):

$$W = \begin{pmatrix} -\frac{1}{2} \\ 1 \end{pmatrix}, D = \begin{pmatrix} d_1 \\ d_2 \end{pmatrix}, \Theta = \theta,$$

434 where $\theta, d_1, d_2 > 0$ are to be specified. Note that either u_2 or u_1 together with u_2 can trigger a spike
 435 in v since $w_{u_1 v} < 0$. Therefore, applying (7) yields that u_2 triggers a spike in v under the following
 436 circumstances:

$$t_v(x) = \theta + t_{u_2} + d_2 \quad \text{if } t_v(x) \leq t_{u_1} + d_1 = x + d_1.$$

437 Hence, this case only arises when

$$\theta + t_{u_2} + d_2 \leq x + d_1 \Leftrightarrow \theta + t_{u_2} + d_2 - d_1 \leq x.$$

438 To emulate f the parameter needs to satisfy

$$\theta + t_{u_2} + d_2 - d_1 \leq x \text{ for all } x \in [0, b] \quad \text{and} \quad \theta + t_{u_2} + d_2 - d_1 > x \text{ for all } x \in [a, 0)$$

439 which simplifies to

$$\theta + t_{u_2} + d_2 - d_1 = 0. \tag{17}$$

440 If the additional condition

$$\theta + t_{u_2} + d_2 = c \tag{18}$$

441 is met, we can infer that

$$t_v(x) = \begin{cases} 2(\theta + t_{u_2} + d_2) - (x + d_1) & , \text{ if } x < 0 \\ \theta + t_{u_2} + d_2 & , \text{ if } x \geq 0 \end{cases} = \begin{cases} -x + c & , \text{ if } x < 0 \\ c & , \text{ if } x \geq 0 \end{cases}.$$

442 Finally, it is immediate to verify that the conditions (17) and (18) can be satisfied simultaneously due
 443 to the assumption that $c > 0$, e.g., choosing $d_1 = d_2 = c$ and $t_{u_2} = -\theta$ is sufficient. \square

444 **Remark 5.** We wish to mention that we can not adapt the previous construction to emulate ReLU
 445 with a consistent encoding scheme, i.e., such that the input and output firing times encode analog
 446 values in the same format with respect to reference times $T_{in}, T_{out} \in \mathbb{R}, T_{in} < T_{out}$. Indeed, it is
 447 obvious that using the input encoding $T_{in} + x$ and output decoding $-T_{out} + t_v$, does not realize
 448 ReLU. Similarly, one verifies that the input encoding $T_{in} - x$ and output decoding $T_{out} - t_v$ also does
 449 not yield the desired function. However, choosing the input encoding $T_{in} - x$ and output decoding
 450 $-T_{out} + t_v$ gives

$$\mathcal{R}_{\Phi}(x) = \begin{cases} -T_{out} - T_{in} + c + x & , \text{ if } x > T_{in} \\ -T_{out} + c & , \text{ if } x \leq T_{in} \end{cases}.$$

451 Setting $T_{in} = 0$ and $T_{out} = c$ implies that Φ realizes ReLU with inconsistent encoding $T_{in} - x$ and
 452 $T_{out} + \mathcal{R}_{\Phi}(x)$. Nevertheless, we want a consistent encoding scheme that allows us to compose ReLU
 453 (as typically is the case in ANNs) whereby an inconsistent scheme is disadvantageous.

454 Applying the previous construction and adding another layer is adequate to emulate f_1 defined in
 455 Proposition 1 by a two-layer SNN.

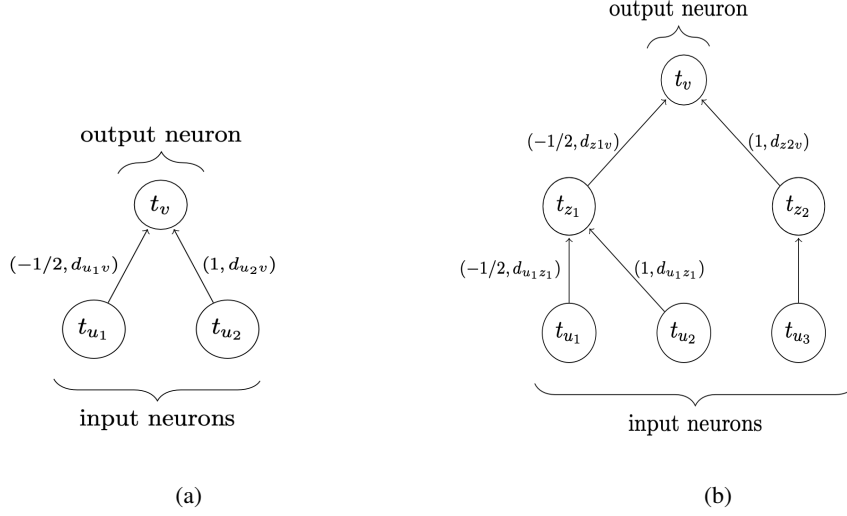


Figure 1: (a) Computation graph associated with a spiking network with two input neurons and one output neuron that realizes f as defined in Proposition 2. (b) Stacking the network in (a) twice results in a spiking network that realizes the ReLU activation function.

456 **Proposition 3.** Let $a < 0 < b < 0.5 \cdot c$ and consider $f : [a, b] \rightarrow \mathbb{R}$ defined as

$$f(x) = \begin{cases} x + c & , \text{ if } x > 0 \\ c & , \text{ if } x \leq 0 \end{cases}$$

457 There exists a 2-layer SNN Φ with output neuron v and input neuron u_1 such that $t_v(x) = f(x)$ on
458 $[a, b]$, where $t_v(x)$ denotes the firing time of v on input $t_{u_1} = x$.

459 *Proof.* We introduce an auxiliary input neuron u_2 with constant firing time $t_{u_2} \in \mathbb{R}$ and specify the
460 parameter of $\Phi = ((W^1, D^1, \Theta^1), (W^2, D^2, \Theta^2))$ in the following manner:

$$W^1 = \begin{pmatrix} -\frac{1}{2} & 0 \\ 1 & 2 \end{pmatrix}, D^1 = \begin{pmatrix} d & 0 \\ d & \frac{d}{2} \end{pmatrix}, \Theta^1 = \begin{pmatrix} \theta \\ 2\theta \end{pmatrix}, W^2 = \begin{pmatrix} -\frac{1}{2} \\ 1 \end{pmatrix}, D^2 = \begin{pmatrix} d \\ d \end{pmatrix}, \Theta^2 = \theta, \quad (19)$$

461 where $d \geq 0$ and $\theta > 0$ is chosen such that $\theta + t_{u_2} > b$. We denote the input neurons by u_1, u_2 ,
462 the neurons in the hidden layer by z_1, z_2 and the output neuron by v . Note that the firing time of
463 z_1 depends on u_1 and u_2 . In particular, either u_2 or u_1 together with u_2 can trigger a spike in z_1
464 since $w_{u_1 z_1} < 0$. Therefore, applying (7) yields that u_2 triggers a spike in z_1 under the following
465 circumstances:

$$t_{z_1}(x) = \theta + t_{u_2} + d \quad \text{if } t_{z_1}(x) \leq t_{u_1} + d = x + d.$$

466 Hence, this case only arises when

$$\theta + t_{u_2} + d \leq x + d \Leftrightarrow \theta + t_{u_2} \leq x. \quad (20)$$

467 However, by construction $\theta + t_{u_2} > b$, so that (20) does not hold for any $x \in [a, b]$. Thus, we
468 conclude via (7) that

$$t_{z_1}(x) = 2(\theta + t_{u_2} + d) - (x + d) = 2(\theta + t_{u_2}) + d - x.$$

469 By construction, the firing time $t_{z_2} = \theta + 2t_{u_2} + d$ of z_2 is a constant which depends on the input
470 only via u_2 . A similar analysis as in the first layer shows that

$$t_v(x) = \theta + t_{z_2} + d \quad \text{if } t_v(x) \leq t_{z_1} + d = 2(\theta + t_{u_2}) + d - x + d = 2(\theta + t_{u_2} + d) - x.$$

471 Hence, z_2 triggers a spike in v when

$$\theta + \theta + 2t_{u_2} + d + d \leq 2(\theta + t_{u_2} + d) - x \Leftrightarrow x \leq 0.$$

472 If the additional condition

$$\theta + t_{z_2} + d = c \Leftrightarrow 2(\theta + d + t_{u_2}) = c \quad (21)$$

473 is met, we can infer that

$$\begin{aligned}
t_v(x) &= \begin{cases} 2(\theta + t_{z_2} + d) - (t_{z_1}(x) + d) & , \text{ if } x > 0 \\ \theta + t_{z_2} + d & , \text{ if } x \leq 0 \end{cases} \\
&= \begin{cases} 2c - (2(\theta + t_{u_2}) + d - x + d) & , \text{ if } x > 0 \\ c & , \text{ if } x \leq 0 \end{cases} \\
&= \begin{cases} x + c & , \text{ if } x > 0 \\ c & , \text{ if } x \leq 0 \end{cases}.
\end{aligned}$$

474 Choosing θ , t_{u_2} and d sufficiently small under the given constraints guarantees that (21) holds, i.e., Φ
475 emulates f as desired. \square

476 **Remark 6.** It is again important to specify the encoding scheme via reference times $T_{in}, T_{out} \in \mathbb{R}$,
477 $T_{in} < T_{out}$ to ensure that Φ realizes ReLU. The input encoding $T_{in} - x$ and output decoding $T_{out} - t_v$
478 does not yield the desired output since it results in a realization of the type $-\text{ReLU}(-x)$. In contrast,
479 the input encoding $T_{in} + x$ and output decoding $-T_{out} + t_v$ with $T_{in} = 0$ and $T_{out} = c$ gives

$$\mathcal{R}_\Phi(x) = -T_{out} + t_v(T_{in} + x) = -T_{out} + f(T_{in} + x) = \begin{cases} x & , \text{ if } x > 0 \\ 0 & , \text{ if } x \leq 0 \end{cases} = \text{ReLU}(x).$$

480 In this case, it is necessary to choose the reference time $T_{in} = 0$ to ensure that the breakpoint is also
481 at zero. Next, we show that there is actually more freedom in choosing the reference time by analysing
482 the construction in the proof more carefully.

483 **Proposition 4.** Let $a < 0 < b$ and consider $f : [a, b] \rightarrow \mathbb{R}$ defined as

$$f(x) = \begin{cases} x & , \text{ if } x > 0 \\ 0 & , \text{ if } x \leq 0 \end{cases}$$

484 There exists a 2-layer SNN Φ with realization $\mathcal{R}_\Phi = f$ on $[a, b]$ with encoding scheme $T_{in} + x$ and
485 decoding $-T_{out} + t_v$, where v is the output neuron of Φ , $T_{in} \in \mathbb{R}$ and $T_{out} = T_{in} + c$ for some constant
486 $c > 0$ depending on the parameters of Φ .

487 *Proof.* Performing a similar construction with the following changes and the same analysis as in the
488 proof of Proposition 3 yields the claim. First, we slightly adjust $\Phi = ((W^1, D^1, \Theta^1), (W^2, D^2, \Theta^2))$
489 in comparison to (19) and consider the network

$$W^1 = \begin{pmatrix} -\frac{1}{2} & 0 \\ 1 & 1 \end{pmatrix}, D^1 = \begin{pmatrix} d & 0 \\ d & d \end{pmatrix}, \Theta^1 = \begin{pmatrix} \theta \\ \theta \end{pmatrix}, W^2 = \begin{pmatrix} -\frac{1}{2} \\ 1 \end{pmatrix}, D^2 = \begin{pmatrix} d \\ d \end{pmatrix}, \Theta^2 = \theta,$$

490 where $d \geq 0$ and $\theta > b$ are fixed (see Figure 1b). Second, we choose the input reference time $T_{in} \in \mathbb{R}$
491 and fix the input of the auxiliary input neuron u_2 as $t_{u_2} = T_{in} \in \mathbb{R}$. Finally, setting the output
492 reference time $T_{out} = 2(\theta + d) + T_{in}$ is sufficient to guarantee that Φ realizes f on $[a, b]$. \square

493 A.5 Realizing ReLU networks by spiking neural networks

494 In this section, we show that an SNN has the capability to reproduce the output of any ReLU network.
495 Specifically, given access to the weights and biases of an ANN, we construct an SNN and set the
496 parameter values based on the weights and biases of the given ANN. This leads us to the desired
497 result. The essential part of our proof revolves around choosing the parameters of an SNN such that
498 it effectively realizes the composition of an affine-linear map and the non-linearity represented by
499 the ReLU activation. The realization of ReLU with SNNs is proved in the previous Section A.4. To
500 realize an affine-linear function using a spiking neuron, it is necessary to ensure that the spikes from
501 all the input neurons together result in the firing of an output neuron instead of any subset of the input
502 neurons. We achieve that by appropriately adjusting the value of the threshold parameter. As a result,
503 a spiking neuron, which implements an affine-linear map, avoids partitioning of the input space.

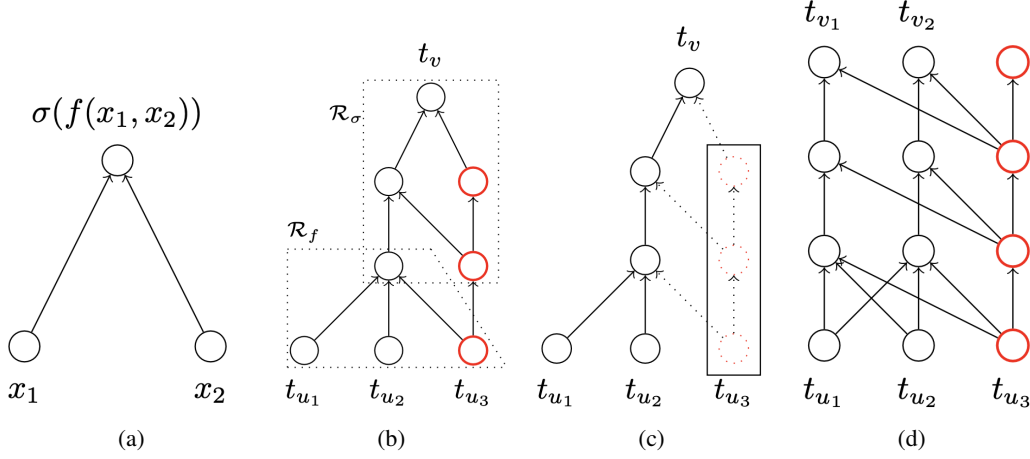


Figure 2: (a) Computation graph of an ANN with two input and one output unit realizing $\sigma(f(x_1, x_2))$, where σ is the ReLU activation function. (b) Computation graph associated with an SNN resulting from the concatenation of Φ^σ and Φ^f that realizes $\sigma(f(x_1, x_2))$. The auxiliary neurons are shown in red. (c) Same computation graph as in (b); when parallelizing two identical networks, the dotted auxiliary neurons can be removed and auxiliary neurons from (b) can be used for each network instead. (d) Computation graph associated with a spiking network as a result of the parallelization of two subnetworks $\Phi^{\sigma \circ f_1}$ and $\Phi^{\sigma \circ f_2}$. The auxiliary neuron in the output layer serves the same purpose as the auxiliary neuron in the input layer and is needed when concatenating two such subnetworks $\Phi^{\sigma \circ f}$.

504 **Setup for the proof of Theorem 3** Let $d, L \in \mathbb{N}$ be the width and the depth of an ANN Ψ ,
505 respectively, i.e.,

$$\Psi = ((A^1, B^1), (A^2, B^2), \dots, (A^L, B^L)), \text{ where } (A^\ell, B^\ell) \in \mathbb{R}^{d \times d} \times \mathbb{R}^d, 1 \leq \ell < L, \\ (A^L, B^L) \in \mathbb{R}^{1 \times d} \times \mathbb{R}.$$

506 For a given input domain $[a, b]^d \subset \mathbb{R}^d$, we denote by $\Psi^\ell = ((A^\ell, B^\ell))$ the ℓ -th layer, where
507 $y^0 \in [a, b]^d$ and

$$y^\ell = \mathcal{R}_{\Psi^\ell}(y^{\ell-1}) = \sigma(A^\ell y^{\ell-1} + B^\ell), 1 \leq \ell < L, \\ y^L = \mathcal{R}_{\Psi^L}(y^{L-1}) = A^L y^{L-1} + B^L \quad (22)$$

508 so that $\mathcal{R}_\Psi = \mathcal{R}_{\Psi^L} \circ \dots \circ \mathcal{R}_{\Psi^1}$.

509 For the construction of the corresponding SNN we refer to the associated weights and delays between
510 two spiking neurons u and v by w_{uv} and d_{uv} , respectively.

511 **Proof of Theorem 3.** Any multi-layer ANN Ψ with ReLU activation is simply an alternating compo-
512 sition of affine-linear functions $A^\ell y^{\ell-1} + B^\ell$ and a non-linear function represented by σ . To generate
513 the mapping realized by Ψ , it suffices to realize the composition of affine-linear functions and the
514 ReLU non-linearity and then extend the construction to the whole network using concatenation
515 and parallelization operations. We prove the result via the following steps; see also Figure 2 for a
516 depiction of the intermediate constructions.

517 **Step 1: Realizing ReLU non-linearity.**

518 Proposition 4 gives the desired result.

519 **Step 2: Realizing affine-linear functions with one-dimensional range.**

520 Let $f : [a, b]^d \rightarrow \mathbb{R}$ be an affine-linear function

$$f(x) = C^T x + s, \quad C^T = (c_1, \dots, c_d) \in \mathbb{R}^d, s \in \mathbb{R}. \quad (23)$$

521 Consider a one-layer SNN that consists of an output neuron v and d input units u_1, \dots, u_d . Via (7)
522 the firing time of v as a function of the input firing times on the linear region R^I corresponding to the

523 index set $I = \{1, \dots, d\}$ is given by

$$t_v(t_{u_1}, \dots, t_{u_d}) = \frac{\theta_v}{\sum_{i \in I} w_{u_i v}} + \frac{\sum_{i \in I} w_{u_i v} (t_{u_i} + d_{u_i v})}{\sum_{i \in I} w_{u_i v}} \quad \text{provided that } \sum_{i \in I} w_{u_i v} > 0.$$

524 Introducing an auxiliary input neuron u_{d+1} with weight $w_{u_{d+1} v} = 1 - \sum_{i \in I} w_{u_i v}$ ensures that
 525 $\sum_{i \in I \cup \{d+1\}} w_{u_i v} > 0$ and leads to the firing time

$$t_v(t_{u_1}, \dots, t_{u_{d+1}}) = \theta_v + \sum_{i \in I \cup \{d+1\}} w_{u_i v} (t_{u_i} + d_{u_i v}) \quad \text{on } R^{I \cup \{d+1\}}.$$

526 Setting $w_{u_i v} = c_i$ for $i \in I$ and $d_{u_j v} = d' \geq 0$ for $j \in I \cup \{d+1\}$ yields

$$t_v(t_{u_1}, \dots, t_{u_{d+1}}) = \theta_v + w_{u_{d+1} v} \cdot t_{u_{d+1}} + d' + \sum_{i \in I} c_i t_{u_i} \quad \text{on } R^{I \cup \{d+1\}} \cap [a, b]^d.$$

527 Therefore, an SNN $\Phi^f = (W, D, \Theta)$ with parameters

$$W = \begin{pmatrix} c_1 \\ \vdots \\ c_{d+1} \end{pmatrix}, D = \begin{pmatrix} d' \\ \vdots \\ d' \end{pmatrix}, \Theta = \theta > 0, \quad \text{where } c_{d+1} = 1 - \sum_{i \in I} c_i,$$

528 and the usual encoding scheme $T_{\text{in}}/T_{\text{out}} + \cdot$ and fixed firing time $t_{u_{d+1}} = T_{\text{in}} \in \mathbb{R}$ realizes

$$\mathcal{R}_{\Phi^f}(x) = -T_{\text{out}} + t_v(T_{\text{in}} + x_1, \dots, T_{\text{in}} + x_d, T_{\text{in}}) = -T_{\text{out}} + \theta + T_{\text{in}} + d' + \sum_{i \in I} c_i x_i \quad (24)$$

$$= -T_{\text{out}} + \theta + T_{\text{in}} + d' + f(x_1, \dots, x_d) - s \quad \text{on } R^{I \cup \{d+1\}} \cap [a, b]^d. \quad (25)$$

529 Choosing a large enough threshold θ ensures that a spike in v is necessarily triggered after all the
 530 spikes from u_1, \dots, u_{d+1} reached v so that $[a, b]^d \subset R^{I \cup \{d+1\}}$ holds. It suffices to set

$$\theta \geq \sup_{x \in [a, b]^d} \sup_{x_{\min} \leq t - T_{\text{in}} - d' \leq x_{\max}} P_v(t),$$

531 where $x_{\min} = \min\{x_1, \dots, x_d, 0\}$ and $x_{\max} = \max\{x_1, \dots, x_d, 0\}$, since this implies that the
 532 potential $P_v(t)$ is smaller than the threshold to trigger a spike in v on the time interval associated
 533 to feasible input spikes, i.e., v emits a spike after the last spike from an input neuron arrived at v .
 534 Applying (5) shows that for $x \in [a, b]^d$ and $t \in [x_{\min} + T_{\text{in}} + d', x_{\max} + T_{\text{in}} + d']$

$$\begin{aligned} P_v(t) &= \sum_{i \in I} w_{u_i v} (t - (T_{\text{in}} + x_i) - d_{u_i v}) + w_{u_{d+1} v} (t - T_{\text{in}} - d_{u_{d+1} v}) = t - d' - T_{\text{in}} + \sum_{i \in I} c_i x_i \\ &\leq x_{\max} + d \|C\|_{\infty} \|x\|_{\infty} \leq (1 + d \|C\|_{\infty}) \max\{|a|, |b|\}. \end{aligned}$$

535 Hence, we set

$$\theta = (1 + d \|C\|_{\infty}) \max\{|a|, |b|\} + s + |s| \quad \text{and} \quad T_{\text{out}} = \theta - s + T_{\text{in}} + d'$$

536 to obtain via (24) that

$$\mathcal{R}_{\Phi^f}(x) = -T_{\text{out}} + t_v(T_{\text{in}} + x_1, \dots, T_{\text{in}} + x_d, T_{\text{in}}) = f(x) \quad \text{for } x \in [a, b]^d. \quad (26)$$

537 Note that the reference time $T_{\text{out}} = (1 + d \|C\|_{\infty}) \max\{|a|, |b|\} + |s| + T_{\text{in}} + d'$ is independent of the
 538 specific parameters of f in the sense that only upper bounds $\|C\|_{\infty}, |s|$ on the parameters are relevant.
 539 Therefore, T_{out} (with the associated choice of θ) can be applied for different affine linear functions as
 540 long as the upper bounds remain valid. This is necessary for the composition and parallelization of
 541 subnetworks in the subsequent construction.

542 **Step 3:** Realizing compositions of affine-linear functions with one-dimensional range and ReLU.
 543 The next step is to realize the composition of ReLU σ with an affine linear mapping f defined in
 544 (23). To that end, we want to concatenate the networks Φ^σ and Φ^f constructed in Step 1 and Step 2,
 545 respectively, via Lemma 1. To employ the concatenation operation we need to perform the following
 546 steps:

- 547 1. Find an appropriate input domain $[a', b'] \subset \mathbb{R}$, that contains the image $f([a, b]^d)$ so that
548 parameters and reference times of Φ^σ can be fixed appropriately (see Proposition 4 for the
549 detailed conditions on how to choose the parameter).
- 550 2. Ensure that the output reference time T_{out}^f of Φ^f equals the input reference time T_{in}^σ of Φ^σ .
- 551 3. Ensure that the number of neurons in the output layer of Φ^f is the same as the number of
552 input neurons in Φ^σ .

553 For the first point, note that

$$|f(x)| = |C^T x + s| \leq d \|C\|_\infty \cdot \|x\|_\infty + |s| \leq d \|C\|_\infty \cdot \max\{|a|, |b|\} + |s| \text{ for all } x \in [a, b]^d.$$

554 Hence, we can use the input domain

$$[a', b'] = [-d \|C\|_\infty \cdot \max\{|a|, |b|\} + |s|, d \|C\|_\infty \cdot \max\{|a|, |b|\} + |s|]$$

555 and specify the parameters of Φ^σ accordingly. Additionally, recall from Proposition 4 that T_{in}^σ can be
556 chosen freely, so we may fix $T_{\text{in}}^\sigma = T_{\text{out}}^f$, where T_{out}^f is established in Step 2. It remains to consider
557 the third point. In order to realize ReLU an additional auxiliary neuron in the input layer of Φ^σ with
558 constant input T_{in}^σ was introduced. Hence, we also need to add an additional output neuron in Φ^f
559 with (constant) firing time $T_{\text{out}}^f = T_{\text{in}}^\sigma$ so that the corresponding output and input dimension and their
560 specification match. This is achieved by introducing a single synapse from the auxiliary neuron in the
561 input layer of Φ^f to the newly added output neuron and by specifying the parameters of the newly
562 introduced synapse and neuron suitably. Formally, the adapted network $\Phi^f = (W, D, \Theta)$ is given by

$$W = \begin{pmatrix} c_1 & 0 \\ \vdots & \vdots \\ c_d & 0 \\ c_{d+1} & 1 \end{pmatrix}, D = \begin{pmatrix} d' & 0 \\ \vdots & \vdots \\ d' & 0 \\ d' & d' \end{pmatrix}, \Theta = \begin{pmatrix} \theta \\ T_{\text{out}}^f - T_{\text{in}}^\sigma - d' \end{pmatrix},$$

563 where the values of the parameters are specified in Step 2.

564 Then the realization of the concatenated network $\Phi^{\sigma \circ f}$ is the composition of the individual realizations.
565 This is exemplarily demonstrated in Figure 2b for the two-dimensional input case. By analyzing
566 $\Phi^{\sigma \circ f}$, we conclude that a three-layer SNN with

$$N(\Phi^{\sigma \circ f}) = N(\Phi^\sigma) - N_0(\Phi^\sigma) + N(\Phi^f) = 5 - 2 + d + 3 = d + 6$$

567 computational units can realize $\sigma \circ f$ on $[a, b]^d$, where $N_0(\Phi^\sigma)$ denotes the number of neurons in the
568 input layer of Φ^σ .

569 **Step 4:** Realizing layer-wise computation of Ψ .

570 The computations performed in a layer Ψ^ℓ of Ψ are described in (8). Hence, for $1 \leq \ell < L$ the
571 computation can be expressed as

$$\mathcal{R}_{\Psi^\ell}(y^{l-1}) = \sigma(A^\ell y^{l-1} + B^\ell) = \begin{pmatrix} \sigma(\sum_{i=1}^d A_{1,i}^\ell y_i^{l-1} + B_1^\ell) \\ \vdots \\ \sigma(\sum_{i=1}^d A_{d,i}^\ell y_i^{l-1} + B_d^\ell) \end{pmatrix} =: \begin{pmatrix} \sigma(f_1(y^{l-1})) \\ \vdots \\ \sigma(f_d(y^{l-1})) \end{pmatrix},$$

572 where $f_1^\ell, \dots, f_d^\ell$ are affine linear functions with one-dimensional range on the same input domain
573 $[a^{\ell-1}, b^{\ell-1}] \subset \mathbb{R}^d$, where $[a^0, b^0] = [a, b]$ and $[a^\ell, b^\ell]$ is the range of

$$(\sigma \circ f_1^{\ell-1}, \dots, \sigma \circ f_d^{\ell-1})([a^{\ell-1}, b^{\ell-1}]^d).$$

574 Thus, via Step 3, we construct SNNs $\Phi_1^\ell, \dots, \Phi_d^\ell$ that realize $\sigma \circ f_1^\ell, \dots, \sigma \circ f_d^\ell$ on $[a^{\ell-1}, b^{\ell-1}]$.
575 Note that by choosing appropriate parameters in the construction performed in Step 2 (as described
576 below (26)), e.g., $\|A^\ell\|_\infty$ and $\|B^\ell\|_\infty$, we can employ the same input and output reference time for
577 each $\Phi_1^\ell, \dots, \Phi_d^\ell$. Consequently, we can parallelize $\Phi_1^\ell, \dots, \Phi_d^\ell$ (see Lemma 2) and obtain networks
578 $\Phi^\ell = P(\Phi_1^\ell, \dots, \Phi_d^\ell)$ realizing \mathcal{R}_{Ψ^ℓ} on $[a^{\ell-1}, b^{\ell-1}]$. Finally, Ψ^L can be directly realized via Step 2
579 by an SNN Φ^L (as in the last layer no activation function is applied and the output is one-dimensional).
580 Although Φ^ℓ already performs the desired task of realizing \mathcal{R}_{Ψ^ℓ} we can slightly simplify the network.

581 By construction in Step 3, each Φ_i^ℓ contains two auxiliary neurons in the hidden layers. Since the
 582 input and output reference time is chosen consistently for $\Phi_1^\ell, \dots, \Phi_d^\ell$, we observe that the auxiliary
 583 neurons in each Φ_i^ℓ perform the same operations and have the same firing times. Therefore, without
 584 changing the realization of Φ^ℓ we can remove the auxiliary neurons in $\Phi_2^\ell, \dots, \Phi_d^\ell$ and introduce
 585 synapses from the auxiliary neurons in Φ_1^ℓ accordingly. This is exemplarily demonstrated in Figure
 586 2c for the case $d = 2$. After this modification, we observe that $L(\Phi^\ell) = L(\Phi_i^\ell) = 3$ and

$$\begin{aligned} N(\Phi^\ell) &= N(\Phi_1^\ell) + \sum_{i=2}^d (N(\Phi_i^\ell) - 2 - N_0(\Phi_i^\ell)) = dN(\Phi_1^\ell) - (d-1)(2 + N_0(\Phi_1^\ell)) \\ &= d(d+6) - 2(d-1) - (d-1)(d+1) = 4d+3 \quad \text{for } 1 \leq \ell < L, \end{aligned}$$

587 whereas $L(\Phi^L) = 1$ and $N(\Phi^L) = d+2$.

588 **Step 5:** Realizing compositions of layer-wise computations of Ψ .

589 The last step is to compose the realizations $\mathcal{R}_{\Phi^1}, \dots, \mathcal{R}_{\Phi^L}$ to obtain the realization

$$\mathcal{R}_{\Phi^L} \circ \dots \circ \mathcal{R}_{\Phi^1} = \mathcal{R}_{\Psi^L} \circ \dots \circ \mathcal{R}_{\Psi^1} = \mathcal{R}_{\Psi}.$$

590 As in Step 3, it suffices again to verify that the concatenation of the networks $\mathcal{R}_{\Phi^1}, \dots, \mathcal{R}_{\Phi^L}$ is
 591 feasible. First, note that for $\ell = 1, \dots, L$ the input domain of \mathcal{R}_{Φ^ℓ} is given by $[a^{\ell-1}, b^{\ell-1}]$ so that,
 592 we can fix the suitable output reference time $T_{\text{out}}^{\Phi^\ell}$ based on the parameters of the network, the input
 593 domain $[a^{\ell-1}, b^{\ell-1}]$, and some input reference time $T_{\text{in}}^{\Phi^\ell} \in \mathbb{R}$. By construction in Steps 2 - 4 $T_{\text{in}}^{\Phi^\ell}$ can
 594 be chosen freely. Hence setting $T_{\text{in}}^{\Phi^{\ell+1}} = T_{\text{out}}^{\Phi^\ell}$ ensures that the reference times of the corresponding
 595 networks agree. It is left to align the input dimension of $\Phi^{\ell+1}$ and the output dimension of Φ^ℓ for
 596 $\ell = 1, \dots, L-1$. Due to the auxiliary neuron in the input layer of $\Phi^{\ell+1}$, we also need to introduce an
 597 auxiliary neuron in the output layer of Φ^ℓ (see Figure 2d) with the required firing time $T_{\text{in}}^{\Phi^{\ell+1}} = T_{\text{out}}^{\Phi^\ell}$.
 598 Similarly, as in Step 3, it suffices to add a single synapse from the auxiliary neuron in the previous
 599 layer to obtain the desired firing time.

600 Thus, we conclude that $\Phi = \Phi^L \bullet \dots \bullet \Phi^1$ realizes \mathcal{R}_{Ψ} on $[a, b]$, as desired. The complexity of Φ in
 601 the number of layers and neurons is given by

$$L(\Phi) = \sum_{\ell=1}^L L(\Phi^\ell) = 3L - 2 = 3L(\Psi) - 2$$

602 and

$$\begin{aligned} N(\Phi) &= N(\Phi^1) + \sum_{\ell=2}^L (N(\Phi^\ell) - N_0(\Phi^\ell)) + (L-1) \\ &= 4d+3 + (L-2)(4d+3 - (d+1)) + (d+2 - (d+1)) + (L-1) \\ &= 3L(d+1) - (2d+1) \\ &= N(\Psi) + L(2d+3) - (2d+2) \end{aligned}$$

603

□

604 **Remark 7.** Note that the delays play no significant role in the proof of the above theorem. Never-
 605 theless, they can be employed to alter the timing of spikes, consequently impacting the firing time
 606 and the resulting output. However, the exact function of delays requires further investigation. The
 607 primary objective is to present a construction that proves the existence of a spiking network capable
 608 of accurately reproducing the output of any ReLU network.